Mausam, (1986), 37, 3, 293-304

551.509.21 : 551.553.21

A short range prediction of the onset phase of the southwest monsoon (1979)

Y. RAMANATHAN*

Atmospheric Environment Service, Montreal, Canada

(*Received 6 November 1984*)

सार — दक्षिण-पश्चिम मानसून (1979) के आरंभिक चरण की प्रागुक्ति के लिए एक भूमण्डलीय मानावलीय निदर्श उपयोग किया गया था। स्रोत सामग्री के रूप में एफ. जी. जी. ई. III–बी एवं मोनेक्स–79 आंकड़ों का सदुपयोग किया गया था। पांच दिन के प्रागुक्ति प्रयोग में लगभग 50° पू० तथा 70° पू० उच्चिष्ठ के साथ पछुआ मानसूनी पवनों का प्रबल होना तथा मानसून धारा की अभिध्रुव की ओर आरंभिक भ्रमिलों का बनना प्रेक्षणों से संगत रूप से मेल खा रहे थे। पांचवें दिन भ्रमिल के उत्तर की ओर जाने तथा अवदाब में परिवर्तित होने की प्रागुक्ति बिल्कुल ठीक की गई थी। निदर्श से प्राप्त परिणामों की भौतिक कार्य प्रणाली जानने की दृष्टि से जांच की गई थी। मानसून गतिविज्ञान में संघननी तापन की भूमिका निर्णायक पाई गई थी। उभरती हुई रेखांशिक दाब प्रवणता तथा क्षेत्रीय पछुआ पवनों के बीच समायोजन प्रक्रियाएं खोजी गई थी। ये प्रक्रियाएं निदर्श निर्गम के बिन्दु निदान विज्ञान में मानसून जेट में स्थित एक बिन्दु 5.0° उत्तर तथा 70° पू० पर पाई गई। ऊर्जा विज्ञान तथा भ्रमिलों की गणना ने दिखाया कि मॉडल वायुमण्डल में भ्रमिल निर्माण में दाब घनत्व संबंधी अस्थिरता ही केवल एक कार्य प्रणाली नहीं हो सकती।

ABSTRACT. A global spectral model was used to predict the onset phase of the southwest monsoon (1979). FGGE III-b and MONEX-79 data sets were used as input. In the 5-day prediction experiment the strengthening of the monsoon westerlies along 5°N with maxima around 50°E and 70°E and the formation of the onset vortex on the poleward side of the monsoon current were in reasonable agreement with the observations. By 5-day the vortex was correctly predicted to move north and form into a depression. The model output was examined to gain an insight into the physical mechanisms. The role of condensational heating in monsoon dynamics was found to be crucial. The adjustment processes between the evolving meridional pressure-gradient and zonal westerlies was traced in the point diagnostics of the model output at a point 5.0°N, 70°E situated in the monsoon jet. Energetics and vorticity computations showed that barotropic instability could not be the sole mechanism in the formation of the vortex in the model atmosphere.

1. Introduction

The onset of the southwest monsoon (referred to hereafter as the monsoon) is known as the burst of the monsoon. Its appearance over the Arabian Sea is often abrupt with the circulation changes which are supposed to be the harbingers of the onset occurring simultaneously or just a few hours before. Two aspects of this burst of the monsoon make it appear spectacular too. One is the strengthening and deepening of the lower tropospheric westerlies over the Arabian Sea. The other is the formation of a disturbance north of the leading edge of the monsoon current, initially as a trough of low pressure, and later developing into a depression on many occasions. This vortex moves north dragging the monsoon current along with it. This study is aimed at providing some understanding of the mechanisms governing these important aspects of the onset phase. The observational studies, based as they are upon poor data coverage especially over the oceanic regions, have been unable to provide explanations for the time-scale and intensity of these transitional onset features. Even the comprehensive data base acquired during the monsoon experiment known as MONEX-79 [Fein and Kuettner 1980] does not seem adequate. However, such data do provide initial and verification observations for numerical models and at this stage, one has, perhaps, to continue to rely on model studies—numerical and theoretical—to probe further into the mechanisms indicated by the observational studies. Some success has already been achieved in simulating the monsoon by general circulation studies (Washington and Daggupaty 1975, Hahn and Manabe 1975[r] and by simpler models [Murakami *et al.* 1970, Godbole 1973, Webster and Chou 1980 a, b, Bannon 1982, Krishnamurti *et al.* 1981]. The role of mechanisms such as differential heating between a heated continent and interactive ocean, hydrological cycle and orographic forcing like that of the Himalayas have been considered in these studies. The conclusions, however, are at variance. This may be, perhaps, due to the neglect of processes in some of these studies so as to keep the models simple. Murakami *et al.* (1970) and Godbole (1973) were able to simulate the onset of monsoon from a dry model including only orography. Their study did not indicate that the hydrological processes were essential. Webster and Chou (1980) on the other hand found that the monsoon onset could be simulated without orography including only the hydrological processes in the model

*Present affiliation : Department of Physics, Indian Institute of Technology, Kanpur, India

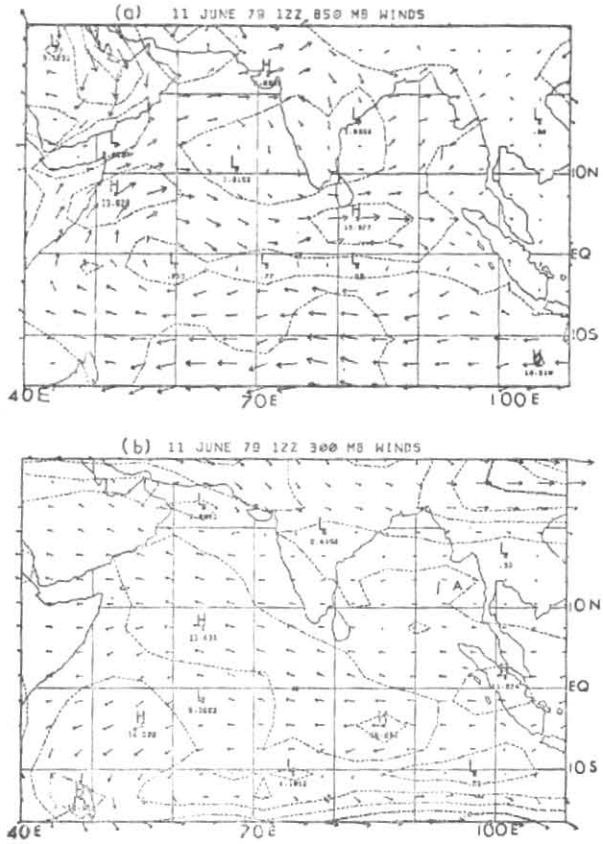

Fig. 1. FGGE III-b analyses of the wind field on 11 June 1979 at 1200 GMT for (a) 850 mb & (b) 300 mb (units : ms^{-1})

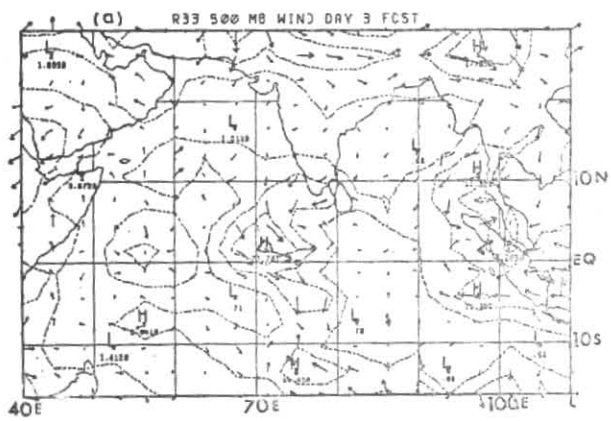

Fig. 2(a). Predicted 3 day 500 mb wind field valid for 14 June 1979, 1200 GMT

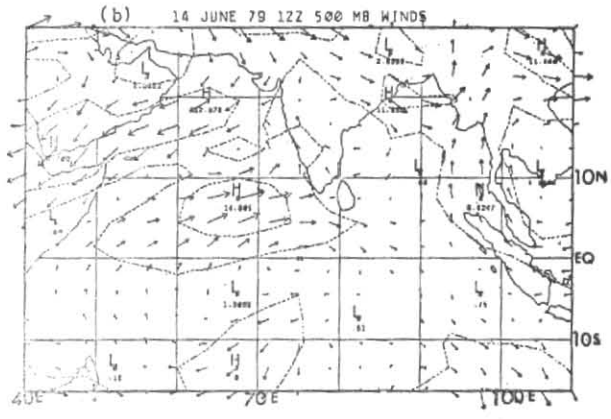

Fig. 2(b). FGGE analyses on 14 June 1979, 1200 GMT at 500 mb

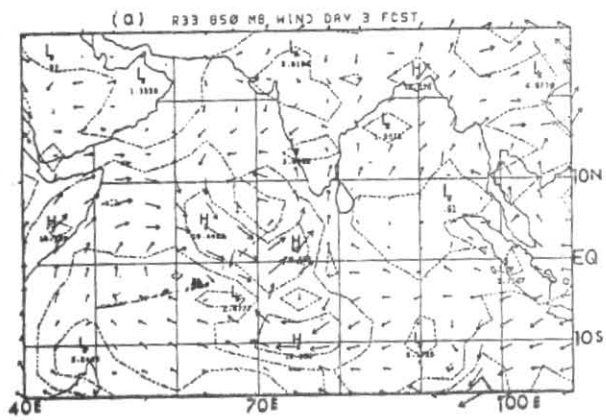

Fig. 3(a). As in Fig. 2(a) except for 850 mb

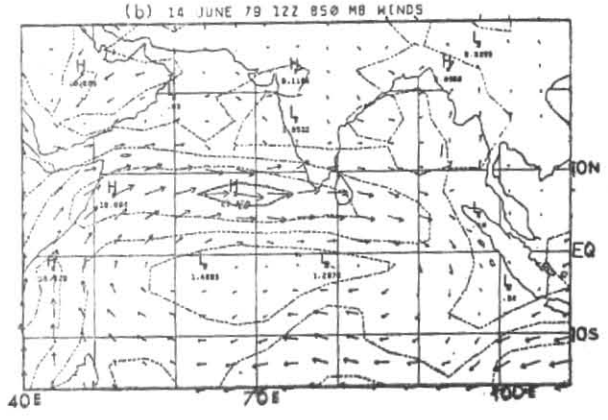

Fig. 3(b). As in Fig. 2(b) except for 850 mb

integrations. Hahn and Manabe (1975) found that both the orographic forcing and hydrological processes were essential. Without mountains, for example, the time-scales of the monsoon transitions like the onset were slower and inconsistent with the observations. Using the MONEX-1979 data sets Krishnamurti *et al.* (1981) calculated that the horizontal shear of the monsoon current could provide substantial energy during the evolution of the onset vortex. The conversion from zonal to eddy kinetic energy was demonstrated by them *via* a simple prediction experiment by simulating the onset vortex from a barotropic model conserving the absolute vorticity. Mak and Kao (1981) agreed that the onset vortex could be accounted for by the process of dynamic instability associated with the horizontal shear. His dry two-layer linear balance model, however, predicted the maximum intensity of the disturbance on the south of the wind maxima in contrast to the observed position of the vortex on the north side. His computations were, however, in agreement with the theoretical work of Kuo (1978) who found that the maximum intensity of the disturbance would occur on that side of the jet where the absolute vorticity was small. The position of the vortex in Krishnamurti *et al.* (1981) was predicted after 48 hours to be at 74° E, 10° N on 15 June '79, 1200 GMT. Though southeast of the observed position at 71°E, 12°N, it was still north of the predicted wind maximum (15.7 m/s at 75°E, 3°N). The question whether the location was predicted on that side of the jet where the absolute vorticity was small was, however, not addressed in their study. Bannon (1982) used a barotropic primitive equation model with bottom friction to simulate the low level monsoon winds from a state of rest. A well-developed monsoon was achieved after a week. No sign of barotropic instability or vortex generation appeared during the model spin-up. Bannon (1982) stated that this discrepancy with those of Krishnamurti *et al.* (1981) may be in the use of bottom friction in his studies and the absence of it in Krishnamurti *et al.* (1981). These two studies, one a simulation from a state of rest and the other a short-range prediction with real data are widely different and may lead to two different monsoon onset flows. It is relevant to point out that the evolution of the monsoon flow was not always preceded by the formation of a vortex (see, Krishnamurti *et al.* 1981 for a summary of occurrences of the onset vortex during 1901-1968). In a later study, Krishnamurti and Ramanathan (1982) examined the sensitivity of the monsoon onset to initially imposed fields of differential heating *via* a multilevel primitive equation model. They traced the evolution of the field of differential heating between land and sea, the consequent build-up of the divergent circulation and the subsequent flow of energy into the rotational component of the wind *via* interactions between the stream function (ψ) and velocity potential (χ). Due to model and data limitations up until now, it has so far not been possible to design short and medium range prediction experiments using real time data sets for the monsoon problem. Since the monsoon is three-dimensional and of planetary scale encompassing both the hemispheres with its characteristic cross-equatorial flow, a global multilevel model becomes a vital necessity. Another essential requirement is representative data sets over equatorial oceanic regions over which the monsoon evolves. With the availability of FGGE III-b data sets and fast computers, designing such prediction experiments have become recently possible. Krishnamurti *et al.* (1983) have reported remarkable success in predicting the formation of a monsoon depression on 4 day and its westward propagation up to 8 day, using a global spectral model having 11 vertical levels with a horizontal resolution of 29 waves in a rhamboidal truncation. The present study is a similar prediction experiment for the monsoon onset phase during 1979 using FGGE III-b data sets. The model specifications and the details of physics are given in section 2. Details of the input data and computations are in section 3. The synoptic history and the evolution of the predicted fields are described in section 4. A discussion of the results follows in section 5.

2. The forecast model

(a) *General particulars*

The global spectral model used in this study is an extension of that of Daley *et al.* (1976). Details of the specifications and the vertical discretization of the basic variables are shown in Appendix I. The prognostic equations of this model are the vorticity, divergence, thermodynamic, mass continuity, moisture conservation and hydrostatic equations. The horizontal representation of variables is described by a truncated series of spherical harmonics, *e.g.*,

$$\phi = \sum_{m=-J}^{J} \sum_{l=|m|}^{J} \phi_l^m \, p_l^m [\sin \alpha] \, e^{im\lambda} \qquad (1)$$

where, m is the zonal wave number,
l is the degree of the associated Legendre function $P(\sin \alpha)$.
α is the latitude and λ is the longitude.

We use a triangular truncation which assumes that the variances contained in scales shorter than the given scales are zero [Baer 1972]. The truncation limit J is set at 39. Non-linear advection terms are calculated by the usual transform method. All of the physical effects like convection and radiation and also the vertical advection terms are computed at grid points of a Gaussian 128 × 60 grid.

The earth's surface ($\sigma = 1$) is a coordinate surface. The mountain height field was truncated to the aforementioned spectral resolution of the model. Semi-implicit time differencing following Robert *et al.* (1972) and a time filtering following Asselin (1972) are used as in Daley *et al.* (1976).

(b) *Model physics*

(i) *Boundary layer*

The model has an elaborate boundary layer formulation which includes the determination of the planetary boundary layer height at each time step. The surface fluxes are calculated by a Businger type formulation based on similarity theory which is discussed by Benoit (1977). The formulation for stable air is empirical and based on experimental data. The model has an explicit formulation for nocturnal inversion based on Delage

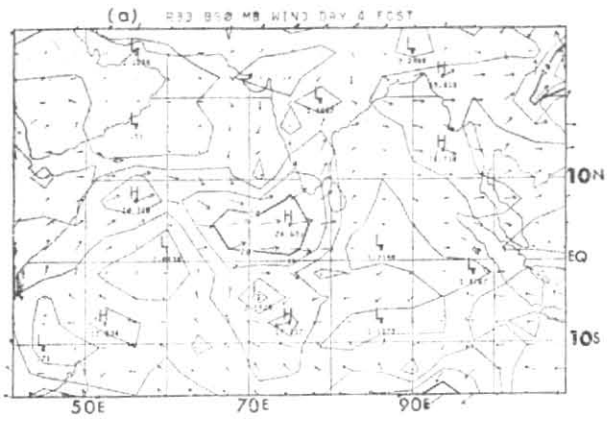

Fig. 4(a). Predicted 4 day 850 mb wind field valid for 15 June 1979, 1200 GMT

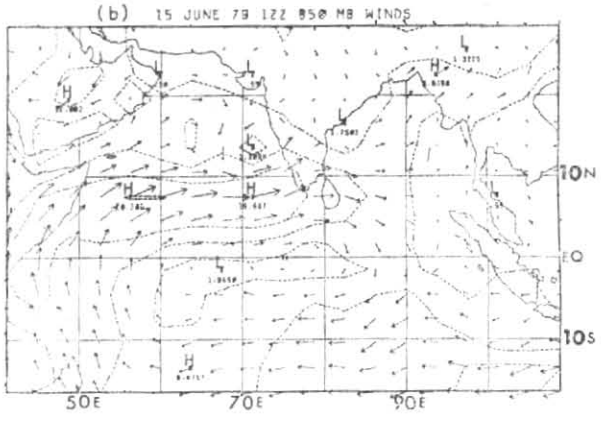

Fig. 4(b). FGGE analysis on 15 June 1979, 1200 GMT at 850 mb

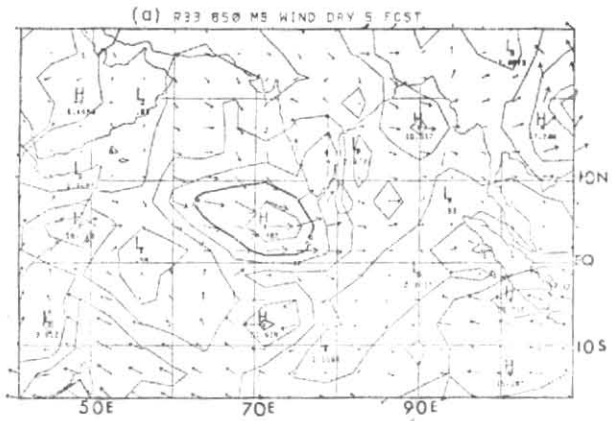

Fig. 5(a). As in Fig. 4(a) except for 5 day and 16 June 1979

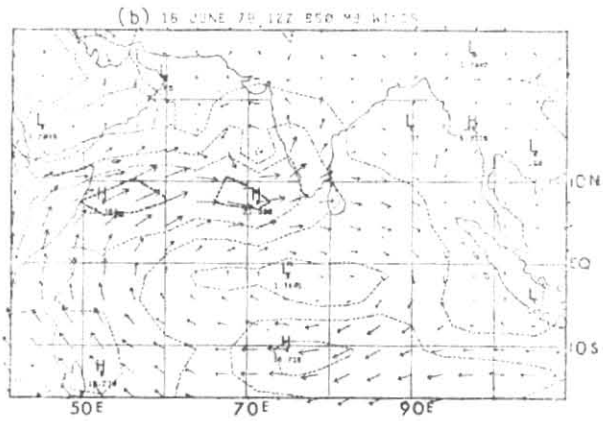

Fig. 5(b). As in Fig. 4 (b) except for 16 June 1979

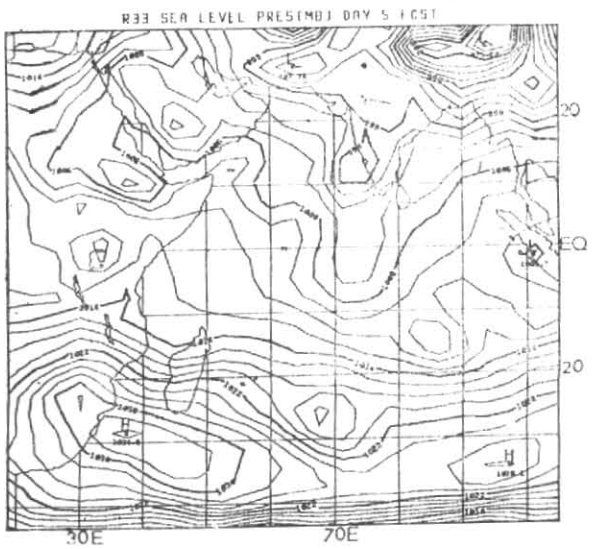

Fig. 6. Predicted 5 day mean sea level pressure (mb) valid for 16 June 1979, 1200 GMT

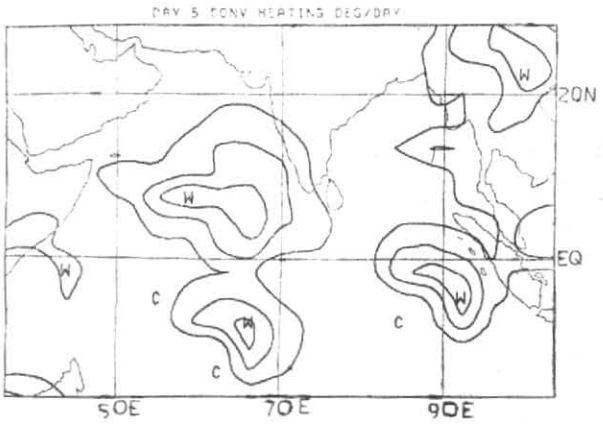

Fig. 7. Condensation heating (Deg. Day^{-1}) computed from predicted rainfall rates for 5 day

(1974). The surface fluxes are extended throughout the planetary boundary layer by a diffusive type formula.

(ii) Radiation

Detailed calculation of radiative transfers of short and long wave irradiances include the effects of cloud feed-back processes, diurnal changes and determination of the heat balance of the earth's surface. The solar heating rates due to absorption by water vapour, ozone and clouds and the flux reaching the ground are calculated using the local zenith angle, cloud distribution and moisture profile. Infra-red fluxes due to water vapour, surface and clouds are calculated using transmissivities for single layers only, keeping the number of operations proportional to the number of levels. Clouds are diagnostically determined at each level from relative humidity and height above the ground. The effect of carbon dioxide is parameterized in the form of heating rates.

(iii) Convection

The treatment of deep cumulus convection is by the scheme in Krishnamurti *et al.* (1976, 1979) which is based on Kuo (1974). In this method a parameter b is defined which partitions the available moisture supply (I) into a large scale moistening part (Ib) and a precipitating part $[(1-b)I]$. The parameter b was found to be near zero in GATE studies by Krishnamurti *et al.* (1980) for the best precipitation rates. In this scheme

$$I = -\frac{1}{g}\int_{p_T}^{p_B} \omega \frac{\partial q}{\partial p}\, dp \tag{2}$$

where p_B is the cloud base which is identified with the lifting condensation level (LCL). p_T denotes the cloud top determined from an intersection of the local moist adiabat (initiated by the lift of air from LCL) with the environmental temperature sounding. Partitioning I we have

$$\begin{aligned} I &= (1-b)I + Ib \\ &= I_\theta + I_q \end{aligned} \tag{3}$$

If Q is the amount of moisture necessary to produce moist adiabatic clouds everywhere inside the grid area and Q_θ, Q_q the heating and moisture parts, we have

$$Q = Q_\theta + Q_q \tag{4}$$

where,

$$Q_\theta = \frac{c_p}{Lg}\int_{p_T}^{p_B}\left[\frac{T_s - T}{\triangle\tau} + \frac{T}{\theta}\,\omega\frac{\partial\theta}{\partial p}\right] dp \tag{5}$$

$$Q_q = \frac{1}{g}\int_{p_T}^{p_B}\left[\frac{q_s - q}{\triangle\tau}\right] dp \tag{6}$$

where $\triangle\tau$ is the cloud time scale taken as 1800 sec in the model. The subscript s denotes a moist adiabat. Let

$$a_\theta = \frac{I_\theta}{Q_\theta} \tag{7}$$

$$a_q = \frac{I_q}{Q_q} \tag{8}$$

Convection is invoked when I is positive, conditional instability is present and there is upward motion. If b is defined, the scheme is closed and a_θ and a_q could be determined so that the large-scale fields are

$$\frac{\partial\theta}{\partial t} = -\mathbf{V}\cdot\nabla\theta - \omega\frac{\partial\theta}{\partial p} + a_\theta\left[\omega\frac{\partial\theta}{\partial p} + \frac{\theta}{T}\frac{c_p}{\triangle\tau}\left(T_s - T\right)\right] \tag{9}$$

$$\frac{\partial q}{\partial t} = -\mathbf{V}\cdot\nabla q + a_q\left[\frac{q_s - c_v}{\triangle\tau}\right] \tag{10}$$

A value of $b = 0.01$ was found to give the best precipitation rates. In this formulation very little moisture goes into storage which is altered mainly by horizontal advection and surface layer fluxes in the regions where convection is invoked. The treatment of large-scale condensation over regions of ascent of stable saturated air and dry convection follow the formulations of Manabe *et al.* (1965).

3. Input to the model and computations

(a) *data*

The observed fields of contour heights (Z), wind (u,v) and relative humidity (RH) were obtained from the FGGE III-b analyses of the European Centre for Medium Range Weather Forecasts (ECMWF). Input to the model at the 15 sigma levels (Appendix 1) were derived from these dats sets. Details of the ECMWF data assimilation system and analysis procedures are described in Bjorheim *et al.* (1981). The model input was for 11 June 1979, and the analysed fields for the period 12-16 June '79 were used for verification purposes. Orography, soil moisture, ice cover, albedo and sea surface temperature fields were climatological and were the same as those used by the Canadian operational weather prediction model (Daley *et al.* 1976). The sea surface temperature field over the Arabian Sea and the adjoining Indian Ocean was, however, reanalysed using MONEX-79 data.

(b) *Initialization*

The model's initialization scheme was based on the nonlinear normal mode initialization procedure in Daley (1979). The number of iterations were limited to three and only the modes with the five largest equivalent depths were adjusted in these integrations.

(c) *Computations*

The model was integrated for 5 days from 11 June '79, 1200 GMT and the output was saved every six hours for computing diagnostic fields.

(i) Condensation heating

Sensible heat, radiation and condensation heating contribute to the net integrated non-adiabatic heating in the model. The evaporative heating is not included since it undergoes a phase change and hence already

gets included in the condensation heating. The condensation heating obtained from the model precipitation rates was found to be almost the sole contributor to the integrated heating. Further discussion on heating is, hence, focussed only on this type.

(*ii*) *Energy parameters*

The basic energy equation follow Lorenz (1967) and Krishnamurti *et al.* (1976). The time evolution of the basic energy parameters and their exchanges were computed over a limited area where the vortex formed. For facilitating comparison the domain chosen was the same 50°E to 70° E and 4° S to 20° N as in Krishnamurti *et al.* (1981). This is not an energy budget but the derivation of the local contributions to global exchanges during the forecast period. The interpretation follows from the studies on regional energetics [Smith 1969]. The computations over the domain are through the depth of the atmosphere from 1000 mb to 100 mb.

(*iii*) *Vorticity*

The vorticity equation in isobaric coordinates is given by

$$\underset{(ZT)}{\frac{\partial \zeta}{\partial t}} = \underset{(HA)}{-\mathbf{V}\cdot\nabla\left[\zeta+f\right]} \underset{(VA)}{-\omega\frac{\partial\zeta}{\partial p}} \underset{(C)}{-\left(\zeta+f\right)\nabla\cdot\mathbf{V}} + \mathbf{k}\cdot\frac{\partial\mathbf{V}}{\partial p}\times\nabla\omega + \left(\mathrm{F}\right) \left(\mathrm{TLT}\right) \qquad (11)$$

where the rate of production vorticity (ZT) is contributed by horizontal advection (HA), vertical advection (VA), generation by horizontal convergence (C), generation by the tilting of the horizontally oriented component of vorticity into the vertical by a non-uniform vertical velocity (TLT) and friction (F). These terms were computed in the southwest (SW), northeast (NE), northwest (NW) and southeast (SE) sectors around the depression during the forecast period. The zone occupied by each sector is a 8° square adjacent to the depression centre (10° N, 70° E).

(*iv*) *Point diagnostics*

The three hourly time history of the evolved fields were saved at a few points over the Arabian Sea for use in the discussion later.

4. Synoptic history and the evolution of the predicted fields

(a) *Synoptic features*

According to Krishnamurti *et al.* (1981) a dramatic increase of westerly kinetic energy started to occur around 11 June 1979 and continued throughout the 5-day period. Their 850 mb analyses for the period 11-16 June '79 show two maxima in the wind field—one around 50° E in the Somali region and the other around 5° N, 70° E. The FGGE III-b analyses also show the establishment of a cross equatorial gyre on 11 June '79 at 850 mb (Fig. 1a) with maxima in the westerlies in the Somali and the central Arabian Sea regions.

The history of the onset vortex, however, seems different in different analyses. To Krishnamurti *et al.* (1981) the vortex was evident earlier at the upper levels prior to its appearance at 850 mb. A closed circulation was found in the data sets around 11 June 1979 at 300 mb and around 13 June '79 at 700 mb but it was not evident at 850 mb until 14 June' 79. Fein and Kuettner (1980) stated that the onset vortex had some of the characteristics of a mid-tropospheric cyclone in the initial stages. The FGGE III-b analyses used in this study give a slightly different picture. There is no evidence of any vortex in the 300 mb wind analysis (Fig.1b) on 11 June '79. 500 mb analysis (Fig. 2b) shows that the vortex first appeared on 14 June which was also seen at 700 mb and 850 mb (Fig. 3b).

(b) *Evolution of the predicted fields*

(*i*) *Monsoon westerlies*

Even in the initial 850 mb chart on 11 June 1979 (Fig. 1a) the cross-equatorial monsoon westerlies had already become established with two distinct maxima, one in the Somali region with a speed of 13.6 ms^{-1} and the other in the equatorial region near Sri Lanka also with a 13.6 ms^{-1} maximum along 5°N. The strengthening of these westerlies was noticed from 3 day onwards. In the Somali region the maxima at 850 mb on 3, 4 and 5 days were observed as 18.9 ms^{-1}, 20.2 ms^{-1} and 22.3 ms^{-1}, respectively. The predicted maxima were 18.7 ms^{-1}, 20.4 ms^{-1} and 18.7 ms^{-1}. Krishnamurti *et al.* (1981) observed that the dramatic formation of the onset vortex was followed by a strengthening of the monsoon westerlies on the equatorside. This increase in the wind speeds was evident in both the observed and predicted 850 mb charts. The observed 3 day to 5 day maxima were 23.4 ms^{-1}, 19.9 ms^{-1} and 21.8 ms^{-1} and the corresponding predicted values were 20.5 ms^{-1} and 24.7 ms^{-1} and 26.4 ms^{-1}. Thus, the 70° E maxima south of the vortex on 4 and 5 days were of greater strength in the predicted charts. Also the monsoon westerlies from the Somali region to 70°E were less continuous and smooth than in the analysed charts and, perhaps, had more small scales than in the analysis. The predicted mean sea level pressure chart on 5 day is shown in Fig. 6. The Mascarene high around 35° S, 35° E intensified and on 3 day a ridge bulged equatorwards from that region in the southern hemisphere. The ridge extended towards the Arabian Sea on the subsequent days with the formation and intensification of a disturbance. The closed isobars of the depression in the Arabian Sea and the monsoon trough along 20° N to 25° N were the prominent features on 5 day.

(*ii*) *The vortex*

The vortex appeared on the predicted and the analysed charts at 500 mb, 700 mb and 850 mb on 3 day (Figs. 2 and 3). The predicted position was north of the leading edge of the monsoon current. The 850 mb location was at 8° N, 69° E which was south of the position 11° N, 69.5° E in the analysis. The analysed charts did not show any significant tilt in the vortex structure with height. The predicted 700 mb and 500 mb positions indicated a southerly tilt of the vortex axis with height at this initial stage. Rao (1976) ascribes this southward slope with height usually observed in the monsoon depressions to the lowest temperatures in the southwest quadrant.

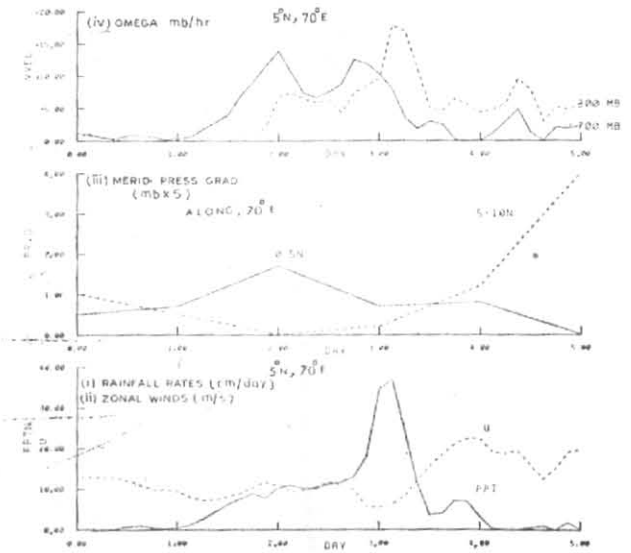

Fig. 8. 3-hour plots of the predicted fields at 5°N,70°E in the monsoon jet. :

(*i*) Rainfall rates (cm day^{-1}),

(*ii*) Zonal wind (ms^{-1}),

(*iii*) Meridional pressure gradients for the latitudinal belts 0°-5°N and 5°-10°N and 5°-10°N computed as difference of mean sea level pressure across a 5-deg. strip (mb×5 deg.),

(*iv*) Omega (mb hr^{-1}) at 700 mb and 300 mb.

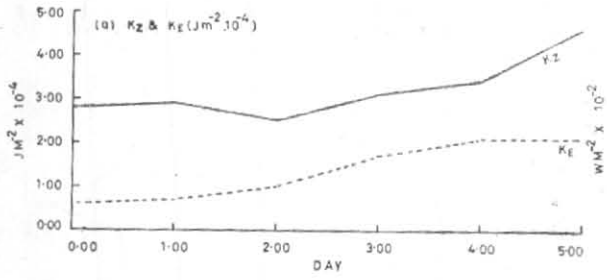

Fig. 9(a). Predicted time variations of energy parameters: Zonal kinetic energy (KZ) and eddy kinetic energy (K_E) for the entire atmosphere

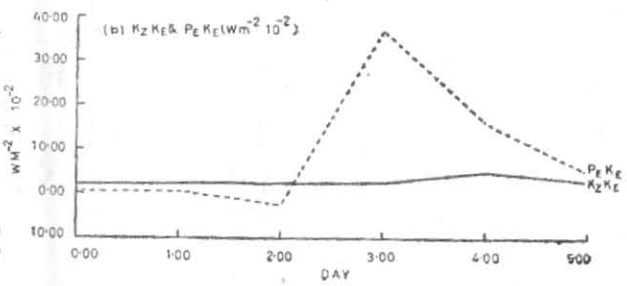

Fig. 9(b). As in Fig. 9(a) except for the energy exchange parameters KZ . K_E and P_E . K_E (units : Wm^{-2} 10^{-2})

The fresh monsoon air in the southwest sector is subjected to lifting in the zone of heavy rains and brings in the lowest temperatures. In the present case the lowest temperatures and the heaviest rainfall were found in the southeast sector. On 4 day (15 June '79) the vortex was found at 11°N, 71°E in the predicted 850 mb chart which was slightly south of the observed position at 12°N, 71°E. The barotropic model prediction of Krishnamurti *et al.* (1981) was more southeasterly at 74°E, 10°N. By 5 day the depression extended upto 300 mb. The predicted disturbance fields showed a south-north movement from 3 day to 5 day which was more gradual at 850 mb than at the higher levels. Such a north-south movement was not apparent in the analysed charts during the five day period.

5. Discussion of the results

(a) *Evolution of the diabatic heating*

It is well-known that the Bay of Bengal branch of the monsoon generally precedes the Arabian Sea branch by a few days. Also the tropical adjustments from winter to summer give rise to widespread thunderstorms in the monsoon region. Sikka and Grossman (1980) reported thundershower activity over Burma and the

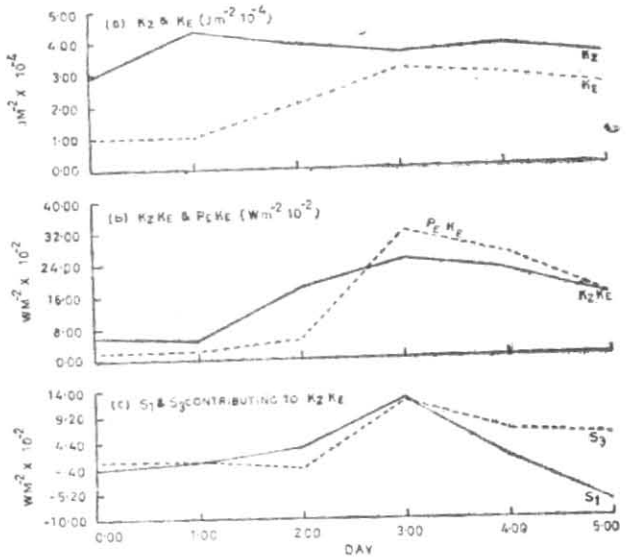

Fig. 10. Predicted time variations of energy parameters : (a) As in Fig. 9(a) except for 100 mb depth centred at 850 mb, (b) As in Fig 10(a) except for the energy exchange parameters $K_Z.K_E$ and $P_E.K_E$ (units : $Wm^{-2}\ 10^{-2}$) and (c) As in Fig. 10 (a) except for the horizontal parameters S_1 and S_3 contributing to $K_Z.K_E$

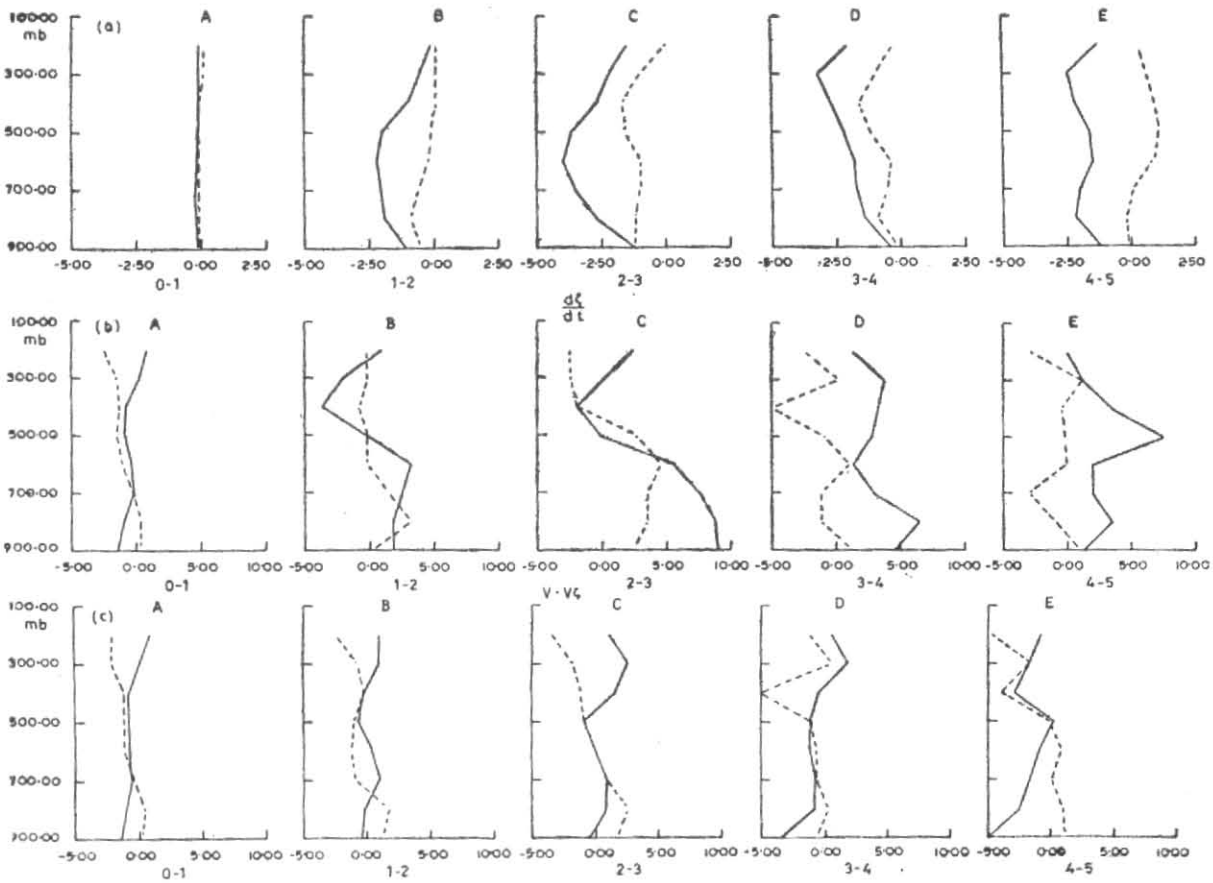

Fig. 11. Predicted vertical profiles

(a) Omega (10^{-3} mb^{-1}) during the days (A) 0-1, (B) 1-2, (C) 2-3, (D) 3-4 and (E) 4-5 in the NW sector (dashed) and SE sector (solid) of the vortex, (b) As in Fig. 11 except for the term vorticity tendency, (VT) (units : $10^{-10}s^{-1}$), (c) As in Fig. 11. except for the term horizontal advection (HA) (units : 10^{-10} s^{-1})

djoining regions from 10 June 1979. The resulting condensational heating forms the bulk of the net integrated heating of the region and is associated with the build-up of the differential heating of the monsoon [Krishnamurti and Ramanathan 1982]. We now describe the evolution of the predicted model condensational heating.

On 2 day a strong zone of heating ($\sim 8°$ C day^{-1}) was found located in the equatorial regions around 95° E. Zonally oriented convective cells ($\sim 6°$ C day^{-1}) were also noticed along the 20°N belt in Burma and the adjoining Indian regions. A northwest-southeast oriented but comparatively weaker cell ($\sim 4°$ C day^{-1}) was also seen along 75° E extending from 10° S to 5°N. On 3 day this 75° E heating intensified ($\sim 12°$ C day^{-1}) and extended further north to 10°N and also westwards to 50° E. The 95° E source was still prominent and it showed only a slight westward movement. On 4 day both the 75° E and 100° E zones of heating showed pronounced meridional orientation. The 75°E cell had extended further north to 15° N. The 5 day heating (Fig.7) was less intense ($\sim 6°$ C day^{-1}). However, the 75° E zone had reached almost upto 20° N.

(b) *Mechanisms for the strengthening of the westerlies*

Investigations of the atmospheric response to heat sources in the equatorial and tropical regions show that there are two distinct physical mechanisms for propagation—the zonally oriented Walker circulation and merdionally propagating monsoon cell or Hadley cell [Webster 1983]. The Walker circulation forced by the equatorial heat source in the mean easterlies such as the one along 95° E in our study was interpreted as Kelvin waves by Webster (1972). Studies by Lim and Chang (1983) show that these transient or pulsating heat sources excite also Rossby wave disturbances which move slowly westward and force further disturbed regions as the one along 75° E. The vertical velocities associated with these heat sources correlated quite well with the regions of heating. A possible mechanism according to Webster (1983) for the northward propagation of the ascending motion is the modulation of the diabatic heating (which is proportional to the vertical velocity distribution) by precipitation and the subsequent changes in the sensible and latent heat fluxes. As the heating moves north, a meridional cross-equatorial pressure gradient builds up as is evident from the mean sea level pressure chart (Fig. 6). Based on trajectory calculations, Kuettner and Unninayar (1980) suggest that the low level monsoon jet over the Arabian Sea is an inertial current streered by the cross-equatorial meriodional pressure gradient. The theoretical conclusion that the latitude reached by a particle released at the equator increases with the pressure gradient is supported by a high correlation between the jet latitude and the different of pressure across the equator. The low level winds, however, in reality do not describe an inertial circle but are driven toward antitriptic balance between pressure gradient, friction and coliolis force. By 11 June both the cross-equatorial gyre and a broad meridional pressure gradient from the southern hemisphere to the northern hemisphere have already been established. The increase in the strength of the westerlies was an adjustment to the increase in the meridional pressure gradient and the northward propagation of the vertical velocity and the precipitation zone. Fig. 8 shows the plots of the condensation heating (precipitation rates) the zonal wind and the vertical velocities at 300 mb and 700 mb across 5° N, 70° E in three-hour intervals from the model output. Also seen the Fig. are the meridional pressure gradients (positive south to north) obtained as differences of the mean sea level pressure across a 5-degree strip in the latitude belts of 0-5°N and 5°-10° N. The precipitation and hence the diabatic heating started increasing from 1 day and reached a maximum on 3 day. The 300 mb vertical velocities also had a maximum around 3 day but the 700 mb vertical velocities reached a maximum value somewhat earlier. This, perhaps, indicated the building up of shallow and later deep clouds in association with the rainfall. During this period the meridional pressure gradient in the 0-5° N belt was greater than that of 5°-10°N but it showed decreasing trend thereafter.

The zonal wind was steady at 10 m/s. After 3 day the precipitation at 5° N, 70° E decreased to insignificant values while the precipitation at 10° N, 70° E started increasing (figure not shown). The meridional pressure gradient in the 5°-10° N belt showed large increase. The zonal wind also increased considerably, perhaps, in response to it. In this process the area of the largest heating moved northwards and closer to the axis of the tropospheric warmest air. This facilitated a more efficient generation of eddy potential energy. The adjustment mechanism would involve the flow of this energy into the divergent part of the wind and then to the rotational part *via* χ-ψ interaction as discussed in detail by Krishnamurti and Ramanathan (1982).

The model output at 5° N, 70° E further indicated that the surface fluxes of moisture and the precipitation rates (verification over the oceanic regions not available) might have been larger than in the real atmosphere. This might have been the reason for the larger than observed values of the meridional pressure gradient in the 5°-10° N belt and the zonal wind at 5°N, 70° E in the predicted 4 day and 5 day 850 mb charts.

(c) *Regional energetics*

The model predictions show that the onset vortex was a three dimensional phenomenon extending upto at least 300 mb by 5 day. To get some insight into the mechanism let us examine some aspects of the regional energetics for the Arabian Sea. Fig. 8 (a, b) shows the time variations of the zonal kinetic energy (K_Z) and the eddy kinetic energy (K_E) and the exchange terms $K_Z.K_E$, and $P_E.K_E$. Both K_Z and K_E showed a monotonic increase from 2 day. The barotropic exchanges ($K_Z.K_E$) though always positive were much smaller than the baroclinic exchanges ($P_E.K_E$) which showed an explosive growth from 2 day to 3 day. Initially $P_E.K_E$ was slightly negative.

The 850 mb energetics showed a different picture (Fig. 10). The K_Z values showed a slight decrease from 1 day to 3 day during which time the K_E values increased substantially (Fig. 10 a). During the build-up stage for the formation of the vortex, some of the K_Z were converted to K_E by the barotropic processes without effecting the available potential energy. The process was achieved

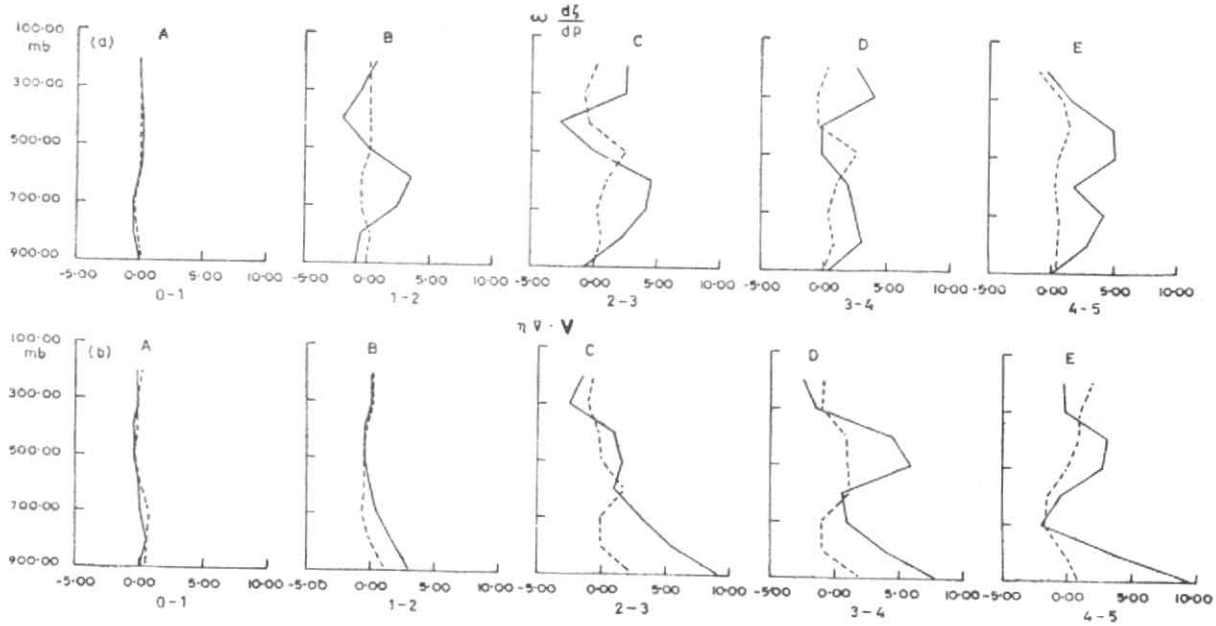

Fig. 12. Predicted vertical profiles

(a) As in Fig. 11 except for the term vertical advection of vorticity (VA) (units : 10^{-10} s^{-2}) and (b) As in Fig. 11 except for the term of convergence producing vorticity (C) (units: $10^{-10} s^{-2}$)

by the horizontal transport of angular momentum by the eddies and are defined by

$$S_1 = -\int_m \left[u' v' \right] \frac{\partial}{\partial y} \left[u \right] \qquad (12)$$

and

$$S_3 = -\int_m \left[u' v' \right] \frac{\partial}{\partial y} \left[v \right] \qquad (13)$$

S_1, S_3 contributions were substantial (Fig. 10 c) for K_Z. K_E exchanges at 850 mb. However, the $P_E.K_E$ were always of comparable magnitudes to $K_Z.K_E$ (Fig.10 b) during the forecast period. If the atmosphere is modelled by a single level, *e.g.*, 850 mb without allowing for any process affecting the available potential energy of the model atmosphere, it is possible that the barotropic exchanges provided by the magnitudes of S_1, and S_3, (Fig. 10 c) could lead to vortex formation as shown by Krishnamurti *et al.* (1981). However, in the present study where the onset vortex is three dimensional and the $P_E.K_E$ term was substantial even at 850 mb, it does not appear that the initiating mechanism was by barotropic processes only.

(d) *Vorticity computations*

An evaluation of the terms of the vorticity Eqn. (11) in the four sectors of the region surrounding the vortex was made. Of all the sectors the SE sector was the most active and the NW sector the least active in building up the onset vortex. Hence the following discussion is confined to these sectors only. Figs. 11 & 12 show the vertical profiles of the omega, vorticity tendency and the production terms, vertical advection, convergence and horizontal advection of the SE and NW sectors.

(*i*) *NW sector* (10°-18° *N*, 62°-70° *E*)

Except on 2 day and 3 day the tendency terms in the NW sector were insignificant. Even on these two days, only the horizontal advection term was building up the cyclonic vorticity in the lower troposphere. The absence of any contributions from the convergence and other terms involving omega indicate that only the barotropic processes could have been important in this sector. The omega values were smaller than those in the SE sector and on 5 day there was also subsidence above 700 mb.

(*ii*) *SE sector* (2°-10° *N*, 70°-78° *E*)

The SE sector was the most active as indicated by the vorticity tendency profiles (Fig. 11 b). Since most of the contributory terms were involving omega, let us first examine the evolution of the omega profiles. Till 3 day the profile maximum was around 600 mb. On 4 day the maximum shifted to 300 mb. From 3 day onwards it appears that deep cumulus convection was dominating this sector. On 5 day the omega profile (Fig.11a) showed two maxima—one in the lower level around 800 mb and the other at 300 mb. The omega structure was seen in the convergence term (Fig. 12 b) which contributed substantially to the vorticity tendency (Fig.11 b). The vertical advection term (Fig. 12 a) was maximum at 600 mb and 700 mb and was, perhaps, the mechanism for middle level cyclogenesis as the convergence term was small at these levels. The horizontal advection terms (Fig.13) were small and were even destructive after 4 day. These computations show no mechanism for the downward propagation of vorticity from the middle to the lower levels. Also the barotropic processes were not significant in this sector for cyclogenesis. The tipping terms were very small in all the sectors and hence their profiles are not shown.

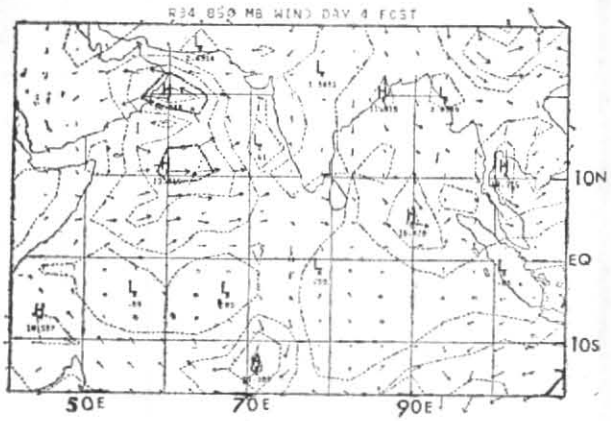

Fig. 13. Predicted 4 day 850 mb wind field valid for 15 June 1979 1200 GMT for the no mountain case

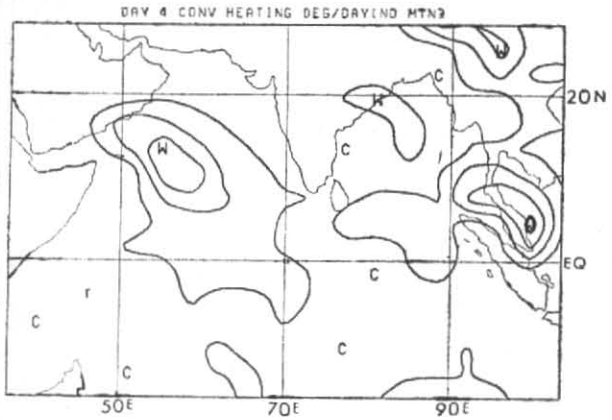

Fig. 14. Predicted 4 day condensation heating (Deg. Day^{-1}) for the no mountain case

(c) *Sub-grid scale contribution*

Vorticity computations were made in the same way as in Daggupaty and Sikka (1977) to assess the role of the sub-grid scale processes in the vorticity balance. The observed tendencies were computed from the FGGE III-b data sets. For the computed tendencies these authors used the omega values from a linear balance model. In our case the model omega values were utilized. The tendencies from observations in both the cases showed significant vorticity generation throughout the troposphere. But the computed tendencies in their case showed vorticity depletion in the middle and upper levels. This descrepancy stressed the existence of an additional sub-grid scale process of the transport of the cyclonic vorticity by deep convective clouds. In the present case the sub-grid scale processes did not appear significant. The onset vortex was like the tropical disturbances in which the net result of the role of convection is to increase the large scale vertical motion with height and thereby increase the cyclonic vorticity. The differences in their structure, the onset vortex over the ocean with a deep layer of convergence and large vertical velocities, and the monsoon depression in the other case over the land with a shallow layer of convergence below 850 mb and a deep layer of weak divergence above, perhaps, emphasize this point.

6. Concluding remarks

A global spectral model with 15 vertical levels and 39 waves was used to predict the onset phase of the south-west monsoon 1979 in a five-day prediction experiment. FGGE III-b and MONEX–79 data sets were used as input to the model. The strengthening of the monsoon westerlies, the formation and the northward movement of the onset vortex were reasonably well-forecast. The role of condensational heating appeared to be crucial. Though barotropic exchanges at the lower levels could be significant for the formation of the onset vortex in a single level integration, in the model the vortex was three dimensional and the $P_E.K_E$ exchanges were comparative to $K_Z.K_E$ even at 850 mb. Barotropic processes alone did not, therefore, seem to be the sole mechanism. The importance of the external forcings such as orography, convection and diffusive processes, the magnitude of which could be critical in the equatorial regions [Webster 1972] have not been separately addressed in this study. Sensitivity experiments on a short or medium range forecast are different from those performed in the general circulation experiments. The data on 11 June 1979 already had many features of the monsoon such as the cross-equatorial gyre and the westerlies over the near-equatorial Arabian Sea. Integration of the model without orography or non-adiabatic heating could not be expected to bring drastic changes. Nevertheless (Fig. 13) which is the 3 day and 4 day 850 mb wind field predicted without the mountains is interesting. The onset vortex formed on 3 day north of the monsoon westerlies but in the west-central Arabian Sea far from the Indian coast and moved towards Arabia rapidly. The associated 4 day condensation heating (Fig. 14) was also close to the Arabian coast and showed a more westward propagation than in the mountain case. It appears that surface hydrology could be enough for the observed features but orography seems necessary for the proper location and movement. These questions will, however, be the subject-matter for a later study.

Acknowledgement

This study was made possible by a fellowship grant from 'The Natural Sciences and Engineering Research Council of Canada'.

References

Asselin, R.A., 1972, Frequency filter for time integration., *Mon. Weath. Rev.*, **100**, 487-490.

Baer,F., 1972, An alternate scale representation of energy atmospheric spectra, *J. atmos. Sci.*, **29**, 649-664.

Bannon, P., 1982, On the dynamics of the east African jet, III: Arabian Sea branch, *J. atmos. Sci.*, **39**, 2267-2278.

Benoit, R., 1977, On the integral of the surface layer profile-gradient function, *J. appl. Met.*, **16**, 859-860.

Bjorheim, K., Julian., P. Kanamitsu. M., Kallberg, P., Price, P., Tracton, S. and Uppala, S., 1981, FGGE III-b daily global analyses, Part 3. ECMWF, Reading, England.

Daggupaty, S.M. and Sikka, D.R., 1977, On the vorticity budget and vertical velocity distribution associated with the life cycle of a monsoon depression, *J. atmos. Sci.*, **34**, 733-792.

Daley, R. C. Girard and Henderson, J., 1976, Short-term forecasting with a multi-level spectral primitive equation model Part I—Model, *Atmos-Ocean*, **14**, 98-116.

Daley, R., and Girard, C., 1979, The application of non-linear normal mode initialization to an operational forecast model, *Atmos. Ocean*, **17**, 98-123.

Delage, Y., 1974, A numerical study of the nocturnal boundary layer, *Quart. J. R. met. Soc.*, **100**, 351-364.

Fein, J. and Kuettner, J., 1980, Report on the summer MONEX field phase, *Bull. Am. met. Soc.*, **61**, 461-474

Godbole, R.V., 1973, Numerical simulation of the Indian summer monsoon, *Indian J. Met. Geophys.*, **24**, 1-14.

Hahn, D.G. and Manabe., S., 1975, The role of mountains in the south-Asian monsoon circulation, *J. atmos. Sci.*, **32**, 1515-1541.

Krishnamurti, T.N., Godbole, R., Chang., C.B., Carr., F. and Chow, J.H., 1976, Study of a monsoon depression (II): dynamical structure, *J. met. Soc. Japan*, **54**, 208-226.

Krishnamurti, T.N., Pan, H., Chang, C.B., Polshay, J. and Oodaly. W., 1979, Numerical weather prediction for GATE, *Quart. J. R. met. Soc.*, **105**, 979-1010.

Krishnamurti, T.N., Ramanathan, Y., Pan. H., Pasch., R. J. and Molinari., J., 1980, Cumulus parameterization and rainfall rates (I), *Mon. Weath. Rev.*, **108**, 465-472.

Krishnamurti, T.N. and Ramanathan, Y., 1982, Sensitivity of the monsoon onset to differential heating, *J. atmos. Sci.*, 39, 1290-1306.

Krishnamurti, T.N., Ardanuy, P., Ramanathan, Y. and Pasch, R.J., 1981, On the onset vortex of the summer monsoon, *Mon. Weath. Rev.*, **109**, 344-363.

Krishnamurti, T.N., Pasch, R. J., Pan, H., Chu, S. H. and Ingles, K., 1983, Details of low latitude medium range weather prediction model I : Formation of a monsoon depression, *J. met. Soc. Japan*, **61**, 188-217.

Kuo, H.L., 1974, Further studies of the parameterization of the influence of cumulus convection on large-scale flow, *J. atmos. Sci.*, **31**, 1231-1240.

Kuo, H.L., 1978, A two-layer model study of the combined barotropic baroclinic instability in the tropics, *J. atmos. Sci.*, **39**, 1290-1306.

Lim, H. and Chang, C.P., 1983, Dynamics of Teleconnections and Walker circulations forced by equatorial heating, *J. Atmos Sci.*, **40**, 1897-1915.

Lorenz, E.N., 1967, *The nature and theory of the general circulation of the atmosphere* published by the World Meteoroloical Organization, Geneva, Switzerland., pp. 1-161.

Mak, M. and Jim Kao, C.Y., 1982, An instability study of the onset-vortex of the southwest monsoon, 1979, *Tellus*, **34**, 358-368.

Manabe, S., Smagorinsky, J, and Strickler, R.F., 1965, Simulated climatology of a general circulation model with hydrologic cycle, *Mon. Weath. Rev.*, **93**, 769-798.

Kuettner, J.P. and Unninayar, M.S., 1980, The near-equatorial jet south of India and its role in the onset of the monsoon FGGE operations Rep. Vol. 9, Results of summer MONEX field phase research., Part B, 96-114, World Meteorological Organization, Geneva, Switzerland.

Murakami, T., Godbole, R.V. and Kelkar, R.R., 1970, Numerical simulation of the monsoon along 80° E., Proc. conf. Summer Monsoon Southeast Asia., C.S. Ramage, Ed., Navy Weather Res. Facility, Norfolk, Va., 39-51, Available from National Technical Information Service, Springfiled. Va, 22161.

Rao, Y.P., 1976, Southwest monsoon, Meteorological monograph: Synoptic Meteorology No. 1/1976, Available from the India Meteorological Department, Lodi Road, New Delhi 110003, India.

Robert, A.J., Henderson., J. and Turnbull, C., 1972, An implicit time integration scheme for baroclinic models of the atmosphere, *Mon. Weath. Rev.*, **100**, 487-490.

Sikka, D.R. and Grossman., R.L., 1980, A chronological weather summary for summer MONEX, FGGE operations report Vol. 8, Summer MONEX field phase report, World Meteorological Organization, Geneva, Switzerland, A2. 1-A2.49.

Smith, P.J., 1969, On the contribution of a limited region to the global energy budget, *Tellus*, **21**, 202-207.

Washington, W.M. and Daggupaty, S.M., 1975, Numerical simulation with the NCAR general circulation model of the mean conditions during the Asian-African summer monsoon, *Mon. Weath. Rev.*, **103**, 105-114.

Webster, P.J., 1972, Response of the tropical atmosphere to local, steady forcing, *Mon. Weath. Rev.*, **100**, 518-541.

Webster, P.J. and Chou, L.C., 1980 (a), Seasonal structure of a simple monsoon system, *J. atmos. Sci.*, **37**, 354-367.

Webster, P.J. and Chou, L.C., 1980 (b), Low-frequency transition of a simple monsoon system, *J. atmos. Sci.*, **37**, 368-382.

Webster, P. J. and Chou, L.C., 1983, Mechanisms of monsoon low frequency variability : Surface hydrological effects, *J. atmos. Sci.*, **40**, 2110-2124.

APPENDIX I

15 Level Spectral Model

Analysis $\phi, u, v, T\text{-}Td$	Prediction ϕ, ζ, D, $T\text{-}Td$
P mb	Sigma
010	0.043
020	0.088
030	0.143
050	0.208
070	0.279
100	0.356
150	0.437
200	0.519
250	0.601
300	0.681
400	0.758
500	0.828
800	0.891
850	0.944
1000	0.985

1. Independent variables	λ, ϕ, σ, t
2. Dependent variables	T (from ϕ), ζ, D, $T\text{-}Td$, Ps, Ts
3. Diagnostic variables	u, v, σ
4. Integration domain	Global
5. Meshwidth	Triangular truncation at wave number 39
6. Grid	60 Gaussian latitudes and 128 longitudes
7. Finite difference	Staggered in the vertical
8. Horizontal diffusion	∇^6 on D, ζ, T, $T\text{-}Td$
9. Time-integration	Semi-implicit ($\triangle t$=20 min)
10. Earth surface	Surface roughness geographically prescribed. Sea surface temperature, soil moisture, snow cover, sea-ice, albedo and deep-soil temperatures analysed for each forecast but constant during the integration
11. Orography	Included consistent with spectral truncation
12. Physical parameterization	(*i*) Boundary layer fluxes of heat, moisture and momentum (*ii*) Kuo's scheme for convection (*iii*) Large scale precipitation (*iv*) Radiation and clouds (*v*) Diurnal cycle.

ϕ = gz
ζ = relative vorticity
D = divergence
$T\text{-}Td$ = dew point depression